

Random Telegraph Signal in Single-Photon Avalanche Diodes

Mohammad Azim Karami¹, Cristiano Niclass², and Edoardo Charbon^{1,2}

¹Faculty of EEMSC, Delft University of Technology, Netherlands

²Department of ECE, Ecole Polytechnic Fédérale Lausanne (EPFL), Switzerland

Tel: (+31) 152783652, Fax: (+31) 152786190, Email: m.a.karami@tudelft.nl

Abstract— Random Telegraph Signal (RTS) behavior is reported in the dark count rate of Single-Photon Avalanche Diodes (SPADs). To the best of our knowledge this is the first time such phenomenon is reported. The RTS characteristics are evaluated experimentally and verified theoretically with respect to bias and temperature.

Index Terms—Random Telegraph Signal, Dark Count Rate, Single Photon Avalanche Diodes

I. INTRODUCTION

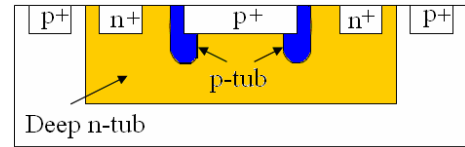
WHENEVER the charge transport through a solid-state device is controlled by the charging and discharging of a single defect, it gives rise to a discrete switching of the current, called burst or popcorn noise, or more often RTS [1]. Although RTS is important for small-area scaled devices, it is shown that the summation of RTSs will result in flicker ($1/f$) noise in large devices [2].

Among solid-state single-photon detectors, CMOS single-photon avalanche diodes (SPADs) are effective in a number of applications, including range-finding, fluorescence detection, and high-speed imaging [3]. A SPAD is generally implemented as a p-n junction biased above breakdown, so as to operate in so-called Geiger mode. Fig. 1. shows the cross-section of a particular implementation of a SPAD in a planar process. In Geiger mode of operation, photo generated carriers may cause an avalanche by impact ionization and correspondingly a current pulse of appreciable amplitude. The operation and properties of SPADs has been studied extensively. See [4] for a review.

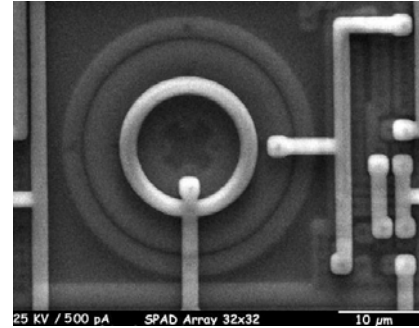
Tunneling, Shockley-Read-Hall (SRH) generation, and afterpulsing are the three main noise sources in SPADs, that can be isolated observing the statistical properties and temperature dependence of the devices [4]. Fig. 2. shows a typical band diagram in a SPAD and an illustration of the first two effects in play. It also shows the functionality of a trap in assisting tunneling and the SRH mechanism. Afterpulsing causes spurious pulse firing following a photon or a dark count, however it can be isolated from the other noise sources by means of output autocorrelation. The noise performance of SPADs is mainly characterized by dark counts which are spurious pulses quantified in terms of mean frequency, or dark count rate (DCR) [5].

DCR bistability is a very interesting effect that directly

relates to the density and distribution of defects in the lattice. Understanding it and modeling it will provide a new tool to predict and analyze defects in standard CMOS processes while providing new techniques to overcome their effects by design. In this paper we describe a temporal fluctuation of DCR between two distinct states. The statistics of such fluctuation follows a RTS behavior.



(a)



(b)

Fig. 1. (a) SPAD cross-section; (b) SEM image of a SPAD implemented in a 0.8μm CMOS process.

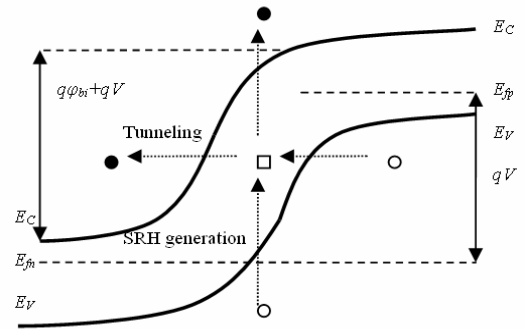


Fig. 2. Band diagram and noise sources of the SPAD under evaluation. V is the reverse applied voltage, E_V is valence band energy, E_C is conduction band energy, and E_F is the Fermi level.

II. RANDOM TELEGRAPH NOISE

RTS phenomena have been observed in currents of MOSFETs, JFETs, DRAMS, proton-irradiated CCDs, neutron irradiated avalanche photodiodes, proton and heavy-ion irradiated active pixel sensors [6, 7]. While the fluctuations in the dark current of imagers are in complex forms such as multi-stable and multi-bistable, the DCR fluctuation in SPADs is one of the rare observations of classical bistable behavior in imagers [8].

A simple two-level RTS is defined by three parameters: the time spent in the up (or high) current state t_u which corresponds to the time during which the trap is empty, the time spent in the down (or low) current state t_d which corresponds to the time during which the trap is filled, and the amplitude [1].

A typical RTS behavior observed in DCR is shown in Fig. 3-a, while Fig. 3-b shows a constant plateau at low frequency and a $1/f^2$ roll off at higher frequencies of the spectral density of the DCR representing the Lorentzian spectrum of RTS noise.

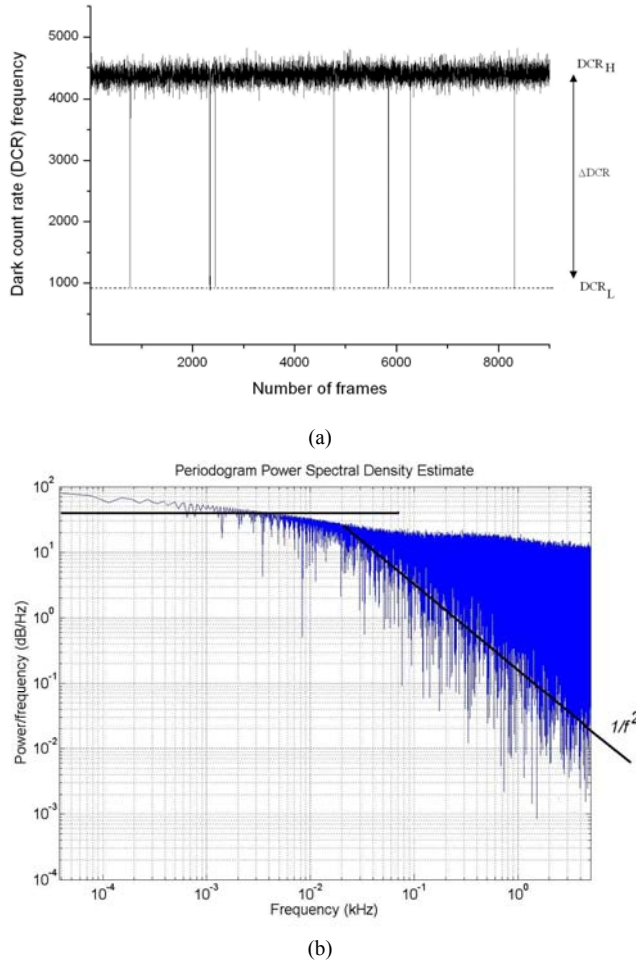


Fig. 3. Bistable DCR levels in a SPAD (a) and Lorentzian noise spectrum of DCR (b).

In addition to analyzing the autocorrelation function, Fig. 3, shows an increase in the probability of RTS occurrence in higher temperatures which is opposite to the afterpulsing

behavior.

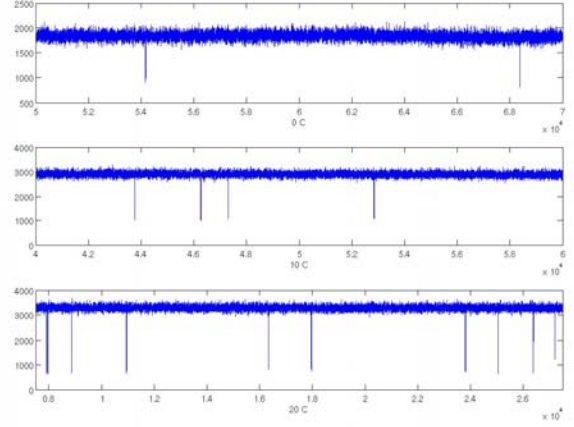


Fig. 4. Temperature dependency of RTS occurrence in 0, 10, and 20 degrees of Celsius.

The measured distribution from a single RTS is exponential, in accordance with a Poisson distribution of random switching events and follows the distribution of the following equation [9].

$$P_{up,down}(t) = \frac{1}{\tau_{up,down}} \exp\left(-\frac{t}{\tau_{up,down}}\right). \quad (1)$$

In this equation the average values of t_u and t_d are given by τ_{up} and τ_{down} and are defined as the up and down time constants. They correspond to the average carrier capture (τ_c) or emission time (τ_e) [2]. Equation (2) shows the dependency of RTS behavior to the biasing conditions [1]. In this equation f_T is the trap occupancy function, g is the degeneracy factor, which is usually considered as unity for electrons, E_T is the trap energy level, k is the Boltzmann constant, E_F the Fermi energy changing with the bias voltage as shown in Fig. 2, and T is the temperature. Moreover, RTS can be induced by surface [9], and bulk defects [6], by the SRH mechanisms and it can also be enhanced by phonon-assisted tunneling, Poole-Frenkel effect, and bistable defect mechanisms [10].

$$\frac{\tau_e}{\tau_c} = \frac{1-f_T}{f_T} = g \cdot \exp\left(\frac{E_T - E_F}{kT}\right). \quad (2)$$

III. RESULTS AND DISCUSSION

In this paper a 32×32 SPAD imager designed and implemented in 0.8 μm CMOS technology is evaluated [3]. The different pixels of the imager show different DCRs corresponding to trap density. Fig. 5. shows the DCR distribution.

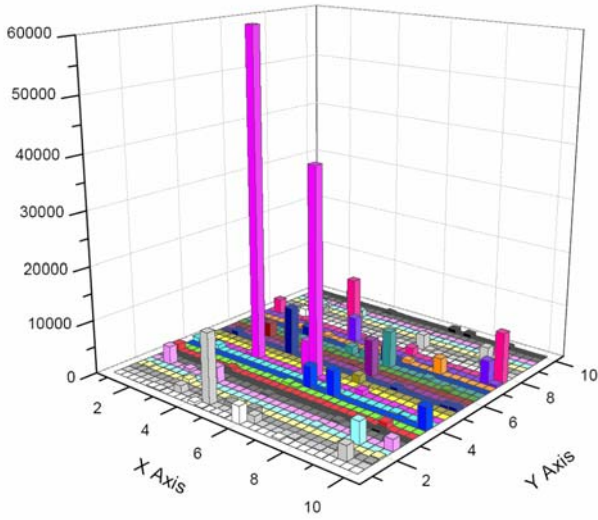


Fig. 5. DCR distribution among the pixels of the 32×32 SPAD array.

The exponential distribution of the time constants agrees with Equation (1) as the characteristic of the RTS noise. A Mean Square Error (MSE) of 0.6 is observed between the theoretical and experimental distribution of RTS as shown in Fig. 6.

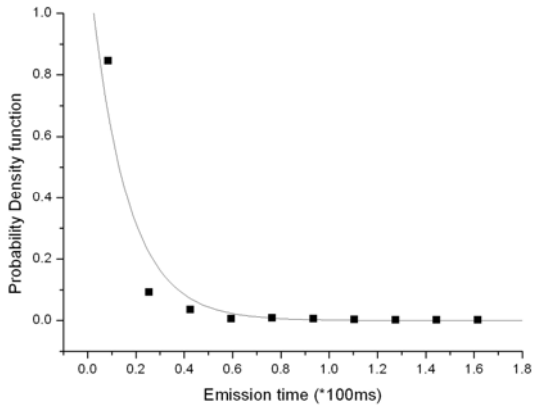


Fig. 6. Comparison between theoretical and analytical probability of the RTS time characteristics.

Fig. 7. shows the dependency of capture (up signal) to the emission (down signal) time versus the excess bias voltage, which is in agreement with Equation (2). Moreover, the large amplitudes of the change in the DCR imply the enhancement of the mechanism of noise generation from the trap.

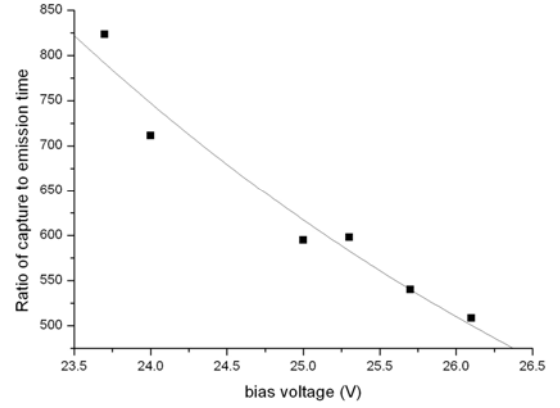


Fig. 7. The ratio of the capture (up) time to the emission (down) time versus the excess bias voltage.

Fig. 8. shows the increase in RTS amplitude as a function of excess bias voltage. This increase on the electric field can be described by considering the trap-assisted tunneling model in which the time constants for tunneling between the valence or conduction band (τ_t) and the trap can be described by Equation (3).

$$\tau_t^{-1} = \frac{qF}{2\sqrt{2m^*}\Delta E} \exp\left(-\frac{8\pi(2m^*)^{1/2}\Delta E^{3/2}}{3qhF}\right). \quad (3)$$

In this equation q is the magnitude of electronic charge, F is the magnitude of electric field at the defect site, m^* is the effective mass for the electron or hole, ΔE is the ionization energy or trap depth, and h is the Planck's constant [11]. DCR would increase rapidly in accordance with decreasing the tunneling time constant between the valence and conduction band.

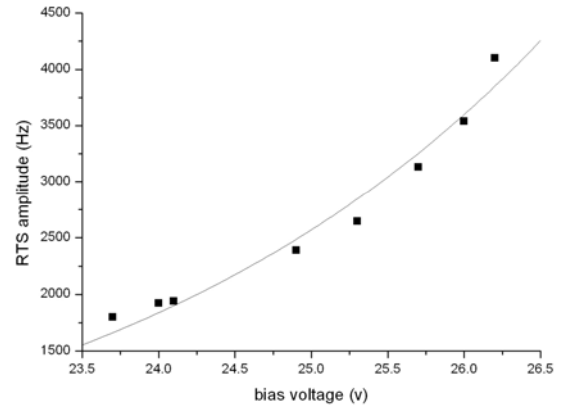


Fig. 8. RTS amplitude (Δ DCR) versus excess bias voltage.

The temperature dependency of capture and emission times is shown in Fig. 9. This temperature behavior is in agreement with the following equation representing the mean times for capture and emission [10].

$$\frac{1}{\tau_{up,down}} = R e^{-E_{act}/kT}, \quad (4)$$

where E_{act} is the activation energy and R is the rate constant, which is different for capture and emission.

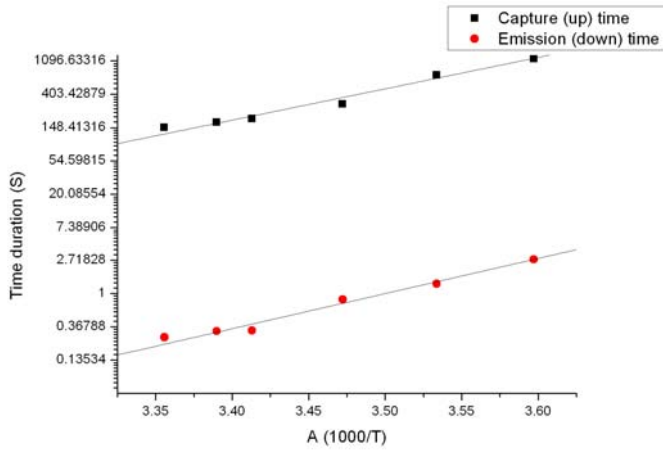


Fig. 9. Temperature dependency of the capture and emission times.

Fig. 10 shows the temperature dependency of RTS amplitude. The one-dimensional Poole Frenkel theory describes the exponential change in the amplitude with respect to temperature by applying factor of χ described in Equation (5) [10]. In this equation k is Boltzmann's constant, ϵ_s is the dielectric constant of silicon, and $|E|$ is the electric field.

$$\chi = \exp(\beta), \beta = \frac{\sqrt{q^3 |E| / \pi \epsilon_s}}{kT}. \quad (5)$$

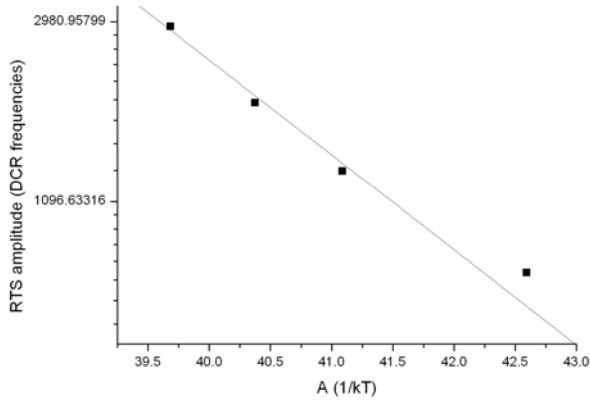


Fig. 10. The RTS amplitude dependency on the temperature.

IV. CONCLUSION

This paper reports on DCR bistability in SPADs. Statistical analysis of the phenomenon reveals that it follows a RTS behavior, similar to current RTS observed in devices where lattice defects are present. The RTS hypothesis was verified by measurements that are in excellent agreement with RTS theory. To the best of our knowledge, this is the first time the effect has been described and modeled.

REFERENCES

- [1] E. Simoen, and C. Claeys, *Materials Science and Engineering B*, **91-92**(30), 136-143 (2002).
- [2] M.J. Kirton, and M.J. Uren, *Adv. in Phys.* **38**, 367-468 (1989).
- [3] C. Niclass, A. Rochas, P.A. Besse, E. Charbon, *J. of Solid-State Circuits*, **40**, 9 1847-1854, (2005).

- [4] A. Rochas, PhD thesis, EPFL, (2003).
- [5] C. Niclass, C. Favi, T.H. Kluter, M. Gersbach, E. Charbon, *Intl. Solid-State circuits conference, ISSCC*, (2008).
- [6] I. H. Hopkins, and G. R. Hopkinson, *Trans. Nuclear Sci.*, **42**(6), 2074-2081 (1995).
- [7] J. Bogarets, B. Dierickx, and R. Mertens, *Trans. Nuclear Sci.*, **49**(1), 249-257 (2002).
- [8] G. R. Hopkinson, V. Goiffon, and A. Mohammadzadeh, *Trans. Nuclear Sci.*, **55**(4), 2197-2204 (2008)
- [9] M.J. Kirton, M.J. Uren, S. Collins, M. Schulz, A. Karmann, and K. Scheffer, *Semicond. Sci. Technol.*, **4**, 1116-1126 (1989).
- [10] I.H. Hopkins, and G. R. Hopkinson, *Trans. Nuclear Sci.*, **40**(6), 1567-1574 (1993).
- [11] G. I. Andersson, M. O. Andersson, and O. Engstrom, *J. Appl. Phys.*, **72**(7), 2680-2691 (1992).